$^{40}Ar/^{39}Ar$ phlogopite geochronology of lamprophyre dykes in Cornwall, UK: new age constraints on Early Permian post-collisional magmatism in the Rhenohercynian Zone, SW England

Nicolle E. Dupuis[1], James A. Braid[1], J. Brendan Murphy[1], Robin K. Shail[2], Doug A. Archibald[3] and R. Damian Nance[4]*

1. *Dept. of Earth Sciences, St. Francis Xavier University, Antigonish, Nova Scotia, Canada, B2G 2W5*
2. *Camborne School of Mines, College of Engineering, Mathematics & Physical Sciences, University of Exeter, Penryn Campus, Penryn, TR10 9FE, UK*
3. *Bruce Wing/Miller Hall, 36 Union St., Queen's University, Kingston, Ontario, Canada, K7L 2N6*
4. *Dept. of Geological Sciences, Ohio University, Athens, Ohio, 45701, USA*

**Corresponding author (e-mail: nicolle.dupuis@gmail.com)*

Abstract

The spatial and temporal association of post-collisional granites and lamprophyre dykes is a common but enigmatic relationship in many orogenic belts, including the Variscan orogenic belt of SW England. The geology of SW England has long been interpreted to reflect orogenic processes associated with the closure of the Rheic Ocean and the formation of Pangea. The SW England peninsula is composed largely of Early Devonian to Carboniferous volcano-sedimentary successions deposited in syn-rift and subsequent syn-collisional basins that underwent deformation and low-grade regional metamorphism during the Variscan orogeny. Voluminous Early Permian granitic magmatism (Cornubian Batholith) is considered to be broadly coeval with the emplacement of lamprophyric dykes and lamprophyric and basaltic lava flows, largely on the basis of geochronological data from lamprophyric lavas in Devon. Although published geochronological data for Cornish lamprophyre dykes are consistent with this interpretation, these data are limited largely to imprecise K-

Ar whole rock and biotite analyses, hindering the understanding of the processes responsible for their genesis and their relationship to granitic magmatism and regional Variscan tectonics.

$^{40}Ar/^{39}Ar$ geochronological data for four previously undated lamprophyre dykes from Cornwall, combined with published data, suggest that lamprophyre magmatism occurred between *c.* 293.6 Ma and *c.* 285.4 Ma, supporting previous inferences that their emplacement was coeval with the Cornubian Batholith. These data provide insights into (i) the relative timing between the lamprophyres and basalts, the Cornubian batholith and post-collisional magmatism elsewhere in the European Variscides, and (ii) the post-collisional processes responsible for the generation and emplacement of lamprophyres, basalts and granitoids.

Introduction

The Upper Palaeozoic Variscan massif of SW England hosts a suite of post-collisional lamprophyric dykes, and lamprophyric and basaltic lavas, that are considered to be approximately coeval with the Early Permian Cornubian Batholith (e.g. Leat *et al.* 1987, Floyd *et al.* 1993; Shail & Wilkinson 1994). There are no exposed contacts between the granites and the lamprophyres or basalts. Although there are high precision U-Pb magmatic monazite / xenotime ages for granites of the Cornubian Batholith (Chen *et al.* 1993; Chesley *et al.* 1993; Clark *et al.* 1994), there are no high precision ages for the lamprophyre dykes, thus precluding evaluation of the temporal relationships between lamprophyric and granitoid magmatism. The only

two high precision age determinations ($^{40}Ar/^{39}Ar$ biotite) are for lamprophyric lavas of the 'Exeter Volcanic Rocks' (Edwards *et al.* 1997), a sequence of lamprophyric and basaltic lavas that occur near the base of Early Permian red bed successions of the Exeter Group in the east of the massif. Lamprophyre dykes intrude Variscan-deformed Devonian and Carboniferous successions throughout the massif, and have been the subject of several geochronological studies (Table 1) that included K-Ar whole rock (Miller *et al.* 1962), K-Ar biotite (Rundle 1980; Rundle 1981), K-Ar phlogopite (Rundle 1980; Hawkes 1981), and $^{40}Ar/^{39}Ar$ plagioclase ages (Roberts 1997). However, the analytical precision is relatively low (2σ typically > 5 Ma) and so the geochronological relationships between the lamprophyre dykes, the dated lamprophyre lavas and the Cornubian Batholith are not adequately constrained.

Genetic linkages between post-collisional mantle and crustal melting have been proposed to explain the common spatial and temporal association of granite batholiths and coeval lamprophyric magmatism (e.g. Scarrow *et al.* 2011; Atherton & Ghani 2002; Fowler & Henney 1996). A mantle component in the Cornubian Batholith has been inferred based on mafic enclave compositions (e.g. Stimac *et al.* 1995), whole rock geochemical and isotopic signatures (e.g. Darbyshire & Shepherd 1994), helium isotope systematics of associated magmatic-hydrothermal mineralisation (Shail *et al.* 2003), as well as the close spatial association with lamprophyres and basalts (Leat *et al*., 1987).

In this paper we present four new $^{40}Ar/^{39}Ar$ phlogopite ages and one $^{40}Ar/^{39}Ar$ whole rock age for previously undated lamprophyre dykes from Cornwall. These data provide further insights into the duration of lamprophyric magmatism in SW England and the relationships between lamprophyres, basalts, granites and local post-Variscan tectonic processes.

Geologic setting

SW England forms part of the European Variscan orogen (Fig. 1) and includes ophiolitic rocks of the Lizard Complex, which suggest proximity to a suture zone that is often referred to as the Rhenohercynian suture (Holder & Leveridge 1986a; Franke 2000; Matte 2001). This region is generally correlated with the Rhenohercynian tectonostratigraphic zone of mainland Europe (e.g. Holder & Leveridge 1986b; Shail & Leveridge 2009; Nance *et al.* 2010; Strachan *et al.* 2013), which extends from the northern margin of the Bohemian massif to the South Portuguese Zone (Fig. 1; Franke 1989).

SW England is interpreted to have resided in the upper plate along the southern flank of Laurussia above a northward-dipping subduction zone during contraction of the Rheic Ocean in the Silurian (e.g. Woodcock *et al.* 2007; Arenas et al. 2014). Collision with the Gondwanan margin at ca. 400 Ma (Nance et al. 2010; Arenas et al. 2014), was followed by opening of the Rhenohercynian Ocean. Most models place SW England on the lower plate during southward subduction that led to the Upper Devonian closure of this ocean (e.g. Holder & Leveridge 1986a; Franke, 2000;

Stampfli et al., 2013). Such a model has been considered to consistent with available data from SW England (Shail & Leveridge 2009).

Despite the lack of exposed autochthonous pre-Devonian rocks, the basement of SW England is traditionally inferred to be of Avalonian affinity based on its position to the north of the Rhenohercynian suture and the demonstrable Avalonian affinity of neighboring crustal blocks in Britain (e.g. Strachan *et al.* 2013). However, the possibility that SW England basement (i.e. to the SW of the Bristol Channel-Bray Fault Zone) might have originated as a separate (non-Avalonian) Gondwana-derived terrane has been raised (Holder & Leveridge 1986b; Woodcock *et al.* 2007; Shail & Leveridge 2009) and a correlation with Meguma has been tentatively suggested (Nance *et al.* 2015).

The Devonian and Carboniferous successions of SW England largely comprise syn-rift marine sedimentary and subordinate volcanic rocks formed on the northern side of the Rhenohercynian marginal basin that was floored, at least locally, farther south by oceanic lithosphere now preserved in the Lizard Complex (ca. 397 ± 2 Ma; Clark et al. 1998; Leveridge & Hartley 2006; Shail & Leveridge 2009). The Gramscatho Basin predominantly comprises syn-convergence deep marine sedimentary rocks deposited during the Upper Devonian closure of this marginal basin (Holder & Leveridge 1986a) and the exposed Culm Basin succession preserves a record of syn-collisional sedimentation up to Moscovian in age (Leveridge & Hartley 2006).

Variscan deformation and low-grade regional metamorphism were diachronous and young progressively from south to north (Holder & Leveridge 1986a; Shail & Leveridge 2009). Regional metamorphic conditions range from upper diagenetic in Upper Carboniferous strata to anchizonal-epizonal in Lower Carboniferous to Lower Devonian strata (Warr *et al*. 1991). ^{40}Ar-^{39}Ar whole rock plateau ages in the Lizard Complex indicate the latter stages of convergence-related deformation / uplift range between 380 Ma and 350 Ma (Clark *et al.* 1998). Farther north, K-Ar whole rock data (Dodson & Rex 1971) for anchizone and epizone rocks in the Gramscatho Basin, recalculated with revised decay constants, and excluding contact metamorphic overprinted samples, yield Famennian to early Tournaisian mean ages of 361 ± 8 Ma (Veryan Nappe) and 358 ± 8 Ma (Carrick Nappe). . Farther north again, anchizonal metamorphism in the Looe Basin has been dated at 331-329 ± 2 Ma (^{39}Ar/^{40}Ar, Clark *et al.* 1998).

The Crediton Graben, which overlies folded and thrusted Holsworthy Group sedimentary rocks of the Culm Basin, initiated by the earliest Permian and contains 'red-bed' successions of the Exeter Group (Fig. 2; Edwards *et al.* 1997). The development of the Crediton Graben reflects the regional transition to a post-Variscan extensional regime manifested by the reactivation of Variscan thrusts, deposition of alluvial/fluvial red-bed sedimentary successions in extensional sedimentary basins and the occurrence of Early Permian mantle-derived magmas (Hawkes 1981; Shail & Wilkinson 1994; Ruffell *et al.* 1995; Shail & Leveridge 2009). The deformed Devonian and Carboniferous successions of the Gramscatho, Looe,

South Devon and Tavy basins were intruded by granites of the Cornubian Batholith between *c.* 293 Ma and *c.* 274 Ma (U-Pb monazite; Table 1; Chesley *et al.* 1993; Chen *et al.* 1993; Clark *et al.* 1994).

Exeter Volcanic Rocks and lamprophyre dykes

The Exeter Volcanic Rocks comprise lamprophyre and basaltic lavas that occur at, or near the base of, the post-Variscan Exeter Group in the Crediton Graben and adjacent areas (Edwards *et al.* 1997; Edwards & Scrivener 1999). Farther north and west, lamprophyre dykes are hosted by Variscan-deformed Devonian and Carboniferous successions (Leat *et al.* 1987; Floyd *et al.* 1993). Both the Exeter Volcanic Rocks and lamprophyre dykes are interpreted to be broadly coeval with the generation and emplacement of the Cornubian Batholith (Leat *et al.* 1987; Edwards *et al.* 1997).

In the Crediton Graben (Fig. 2) the lamprophyre lavas, are locally succeeded by shoshonitic and olivine basalt lavas; all are interbedded with Early Permian 'red-bed' alluvial/fluvial sedimentary rocks (Tidmarsh 1932; Thorpe *et al.* 1986; Edwards & Scrivener 1999). The Early Permian age of lavas in the Crediton Graben is broadly constrained by a Moscovian fossil assemblage in the underlying deformed and very low-grade regionally metamorphosed Holsworthy Group (Waters *et al.* 2011) and by Late Permian miospores from the overlying upper part of the Exeter Group (Warrington & Scrivener 1990; Edwards *et al.* 1997). Lamprophyric and basaltic lavas crop out over a total area of approximately 6 km^2 but aeromagnetic

anomalies suggest that much of the Crediton Graben may be underlain by fully concealed lavas (Edwards & Scrivener 1999). The lamprophyre lavas are minettes and, less commonly, kersantites usually composed of phlogopite/biotite, olivine, pyroxene, apatite, alkali feldspar and/or plagioclase. Alteration is prevalent and primary minerals have largely been replaced by carbonates and Fe-oxides. The lamprophyres generally form flows on the order of tens of metres thick, however it is possible that some are high-level intrusive sills (e.g. Floyd *et al.* 1993; Edwards & Scrivener 1999). The basalt lavas are variably vesicular, highly altered alkali basalts that form flows 20-30 m thick. They are generally composed of pseudomorphed olivine, pyroxene, plagioclase, ilmenite, calcite, chlorite and quartz. Detailed petrographic descriptions have been provided by Edwards & Scrivener (1999), Floyd *et al.* (1993) and Fortey (1991).

High precision ^{40}Ar-^{39}Ar biotite cooling ages of 290.8 ± 0.8 Ma have been reported for the extrusive Killerton minette and 281.8 ±0.8 Ma for a lamprophyre lava known as the Knowle Hill olivine microsyenite exposed in the Crediton Graben (Fig. 2) (Edwards *et al*. 1997; Edwards & Scrivener 1999).

The lamprophyre dykes are variably oriented, generally >1 m wide, and post-date Variscan convergence-related fabrics in their Devonian to late Carboniferous host successions (Table 2; e.g. Smith 1929; Hall 1982; Leat *et al.* 1987; Floyd *et al.* 1993). Although almost all lamprophyre dykes crop out within 25 km of the Cornubian Batholith margin, in a so-called 'shadow zone', there are no occurrences of cross-

cutting relations with either the granites or their metamorphic aureoles (Leat *et al*. 1987). The dykes, like the extrusive lamprophyres of the Exeter Volcanic Rocks, are minettes or kersantites and most are extensively altered. Quartz xenocrysts and xenoliths of host rock, lamprophyric material, quartz vein and granite are common.

Geochronological data for the lamprophyre dykes are sparse and are limited to imprecise K-Ar data (Miller *et al.* 1962; Rundle 1980; Rundle 1981) that yield ages ranging from *c.* 300 Ma to *c*. 285 Ma (Table 1). An ^{40}Ar-^{39}Ar plagioclase cooling age of 292.4 ± 7.1 Ma has been reported for the Fremington kersantite dyke (Table 1; Roberts 1997), which intrudes Tournaisian strata (Pilton Shale Group) in the uppermost succession of the North Devon Basin (Fig. 2; Leveridge & Hartley 2006).

The lamprophyre lavas and dykes are highly enriched in incompatible and light rare earth elements (LREE) and have isotopic compositions characteristic of a previously metasomatised sub-continental lithospheric mantle source (Grimmer & Floyd 1986; Leat *et al.* 1987; Floyd *et al.* 1993).

Sample descriptions

Almost all lamprophyre dykes in Cornwall and described in this study are shown on British Geological Survey 1:50 000 maps. Some lamprophyre exposures implied on maps derived from 'first edition' mapping (*c.* 1900-1910) are no longer extant or accessible. Other extant exposures, such as the Holywell lamprophyre (NED04) and those farther north around Newquay, are shown on 'first edition' maps but not on

maps published following more recent 'second edition' mapping (cf. BGS 2012 with GSGB 1906). Photomicrographs and photographs of sample locations are provided in the Supplementary Publication.

Sampling targets were selected from BGS maps and memoirs (Table 2) and were dykes for which no geochronological data are available. Four relatively unaltered, coarse grained, porphyritic lamprophyre dykes were chosen for geochronological analysis based on availability and quality of mica separates. One fine-grained dyke was selected for whole-rock $^{40}Ar/^{39}Ar$ analysis to compare with the mica separates. All samples described in this paper were processed for zircon separates but no zircon was recovered, although zircon was identified by electron microprobe in one sample (NED07). Therefore, we use $^{40}Ar/^{39}Ar$ geochronology to determine the age of emplacement. We consider this method reliable because the lamprophyres are relatively thin dykes that intruded low-grade, upper crustal sedimentary successions, outside the contact metamorphic aureole of the Cornubian Batholith, and would therefore have cooled through the mica blocking temperature shortly after emplacement.

NED01 and NED 03

Sample NED01 was collected from a ~1 m wide lamprophyre dyke that crops out on the shoreline of the Helford Estuary, accessible only at low tide. Sample NED03 was collected from a ~1.5 m wide dyke that crops out on the east bank of Frenchman's Creek, approximately 500 m west of Helford village (Fig. 2). Both are hosted by the

Upper Devonian Portscatho Formation of the Gramscatho Basin (Table 1; Leveridge & Hartley 2006; Leveridge & Shail 2011) and are weathered to a rusty red color; they are likely to represent exposures of the same dyke, with approximately 800 m along-strike separation. Both exhibit porphyritic texture, with mica phenocrysts in a groundmass of alkali feldspar, augite, apatite, titanite, rutile and barite. Hydrothermal alteration is evidenced by the presence of calcite, iron-titanium oxides, iron carbonates, sericitization of feldspars and minor chloritization along the edges of some phlogopite grains. Mica separated from both samples for $^{40}Ar/^{39}Ar$ analysis is generally euhedral, dark brown and 0.5 to 1.5 mm in length.

NED04

Sample NED04 is from a lamprophyre dyke that crops out on the NE side of Holywell Beach, where it is hosted by the Lower-Upper Devonian Trendrean Mudstone Formation (Meadfoot Group) of the Looe Basin (Leveridge 2011; Hollick *et al.* 2014). The dyke varies in width from approximately 3-5 m and is exposed in the cliff face where it is accessible at low tide. It is very fine grained relative to other analyzed samples and is more pervasively altered.

NED07

This sample was obtained from a ~1 m wide lamprophyre dyke that intruded the Portscatho Formation (Upper Devonian) at Pendennis Point, near Falmouth (Fig. 2) and has previously been described by Hall (1982). The dyke is well exposed at low tide and can be traced around Pendennis Point. Several cm-scale dykes branch from

the main intrusion. Post-emplacement sinistral movement is evident from metre-scale offsets of the dyke contacts with the host rock. The dyke is very similar in mineralogy and texture to NED01 and NED03 and contains mica phenocrysts in a groundmass of alkali feldspar, mica, titanite, barite, alkali amphibole and rutile (Hall 1982). Calcite, iron oxides and iron carbonates are the dominant secondary phases. Zircon and monazite (both too small to be precisely dated) are also present in small quantities, as well as resorbed quartz interpreted to be of xenocrystic origin. The Na-rich richterite documented by Hall (1982) was not observed in this study.

NED12

Sample NED12 is from a lamprophyre dyke that crops out on the bank of the River Fal approximately 1 km south of the Trelissick Garden in Feock (Fig. 2). This lamprophyre forms a gently dipping ~2 m wide dyke that intrudes the Upper Devonian Portscatho Formation and is well exposed at low tide. It has the same mineral assemblage and porphyritic texture as NED01 and NED03, however the micas are generally black, rather than dark brown.

Mica composition

Prior to Ar-Ar analysis, mica phenocrysts were analyzed in situ in polished thin sections using a JEOL 8200 electron microprobe at the Robert MacKay Electron Microprobe Laboratory, Dalhousie University.

Micas in samples NED01 (Fig. 3a) and NED03 (Fig. 3b) are phlogopite with moderate variation in Al^{IV} (1.67-2.26) and slight variation in Mg# (0.83-0.89). Sample NED07 (Fig. 3c) contains both phlogopite and Mg-rich biotite and the majority of micas are zoned, generally with pale brown cores and dark brown rims. The Mg# for micas in sample NED07 varies from 0.65 to 0.94 and Al^{IV} ranges from 1.48 to 1.89. Sample NED12 (Fig. 3d) also contains both phlogopite and Mg-rich biotite (Mg# = 0.66-0.86; Al^{IV} = 1.76-2.07). Complete electron microprobe data and calculated number of ions per formula are provided in the Supplementary Publication.

Analytical techniques

Several kilograms of sample were taken from each location (Table 2). Samples were processed in a jaw crusher and sieved to <1 mm at the University of Portsmouth, UK. Phlogopites were then handpicked from the <1 mm sieve fraction for irradiation and $^{40}Ar/^{39}Ar$ analysis. One sample (NED04) was too fine grained to yield a phlogopite mineral separate, so whole rock $^{40}Ar/^{39}Ar$ analysis was performed instead.

Mineral separates and flux-monitors (standards) were wrapped in aluminium foil. The resulting disks were stacked vertically into an 8.5 cm long and 2.0 cm diameter aluminium irradiation capsule, and then irradiated with fast neutrons in position 8C of the McMaster Nuclear Reactor (Hamilton, Ontario) for a duration of 72 hours (at 3 MWH). Packets of flux monitors were located at ~0.5 cm intervals along the irradiation container and the J-value for an individual sample was determined by

least-squares, second-order polynomial interpolation using replicate analyses of splits for each monitor position in the capsule.

The irradiated samples were loaded into flat-bottomed pits in a copper sample-holder and placed beneath the ZnS view-port of a small, bakeable, stainless-steel chamber connected to an ultra-high vacuum purification system. Following bake out at 100°C, a 30 watt New Wave Research MIR 10-30 CO_2 laser with a faceted lens was used to heat samples for ~3 minutes at increasing percent power settings (2% to 45%; beam diameter 3 mm). After purification using hot and cold SAES C50 getters (for ~5 minutes), the evolved gas was admitted to an MAP 216 mass spectrometer, with a Bäur Signer source and an analogue electron multiplier (set to a gain of 100 over the Faraday detector).

Measured argon-isotope peak heights were extrapolated to zero-time and corrected for discrimination using a $^{40}Ar/^{36}Ar$ atmospheric ratio of 295.5 and measured ratios of atmospheric argon. Blanks, measured routinely, were subtracted from the subsequent sample gas-fractions. The extraction blanks are typically $<10 \times 10^{-13}$, $<0.5 \times 10^{-13}$, $<0.5 \times 10^{-13}$, and $<0.5 \times 10^{-13}$ cm^{-3} STP for masses 40, 39, 37, and 36, respectively. ^{39}Ar and ^{37}Ar were corrected for radioactive decay during and after irradiation. Corrections were made for neutron-induced ^{40}Ar from potassium, ^{39}Ar and ^{36}Ar from calcium, and ^{36}Ar from chlorine (Roddick 1983; Onstott *et al.* 1991). Dates and errors were calculated using the procedure of Dalrymple *et al.* (1981) and the constants of Steiger & Jäger (1977). Plateau and inverse isotope correlation

dates were calculated using ISOPLOT v. 3.60 (Ludwig 2008). A plateau is herein defined as three or more contiguous steps containing >50% of the ^{39}Ar released, with a probability of fit > 0.01 and MSWD < 2. If a date is defined by contiguous steps containing <50% of the ^{39}Ar released, it is referred to as a plateau segment age.

Errors shown in the tables and on the age spectra and inverse isotope correlation diagrams represent the analytical precision at 2σ, assuming that the errors in the ages of the flux monitors are zero. This is suitable for comparing within-spectrum variation and determining which steps form a plateau (e.g. McDougall & Harrison 1988). The dates and J-values are referenced to GA-1550 biotite (98.79 Ma; Renne *et al.* 1998) and Hb3Gr hornblende (PP-20; 1073.6 Ma; Jourdan *et al.* 2006).

Results

A summary of the $^{40}Ar/^{39}Ar$ data is shown in Table 3. Complete data sets are in the Supplementary Publication. Step heating of phlogopite separates resulted in release patterns with initially low ages, increasing quickly but irregularly to a well-defined plateau (Fig. 4a-d). NED01 yielded a sixteen-step plateau (Fig. 4a) with 95.3% of the ^{39}Ar, with a plateau age of 287.42 ± 0.61 Ma, and a high-T plateau segment age of 287.59 ± 0.68 Ma (^{39}Ar= 88.4%). NED01 was the only sample to yield a meaningful inverse isochron (Fig. 4b), which suggests the absence of excess Ar (e.g. Kuiper 2003) and indicates an age of 288.0 ± 2.1 Ma. Sample NED03 produced a thirteen-

step plateau (Fig. 4c) with an age of 285.74 ± 0.66 Ma (76.8% of the ^{39}Ar) and a high-T plateau segment age of 284.38 ± 1.07 Ma (^{39}Ar= 35.4%). Sample NED07 produced an age of 295.03 ± 0.77 Ma from the eleven-step plateau (65.4% of the ^{39}Ar; Fig. 4d) and a high-T plateau segment age of 292.1 ± 1.5 Ma (^{39}Ar= 23.8%). Finally, NED12 produced an eleven-step plateau (Fig. 4e), with 79.5% of the ^{39}Ar, that yielded an age of 287.91 ±0.71 Ma and a high-T plateau segment age of 286.9 ± 1.54 Ma (^{39}Ar= 19.0%).

Step heating of the whole-rock sample NED04 resulted in a hump-shaped release pattern. A whole-rock plateau age of 262.1 ± 1.3 Ma that represents 52.6% of the ^{39}Ar, and a high-T plateau segment age of 248 ± 3.6 Ma (^{39}Ar= 11.3%) was obtained from this sample (Fig. 4e).

The presence of chlorite in biotite or phlogopite separates, in addition to ^{39}Ar recoil loss, has been shown to produce anomalously old ^{40}Ar/Ar^{39} ages, which are often characterized by distinct hump- or saddle-shaped plateau spectra (e.g. diVincenzo *et al.* 2003; Paine *et al.* 2006). Low- to mid-T humps are present in all samples except NED01 and are likely a result of interlayered chlorite and ^{39}Ar recoil loss during irradiation. Therefore, it is likely that the calculated plateau ages are in excess of the true cooling ages (e.g. diVincenzo *et al.* 2003; Paine *et al.* 2006) and that the high-T plateau segment dates reflect the true cooling ages of the phlogopites, and so we use these ages for geological interpretations.

Discussion

The four ^{40}Ar-^{39}Ar phlogopite ages presented are the first high precision geochronological data available for lamprophyre dykes in Cornwall. They represent intrusion ages between 292.10 ± 1.5 Ma and 284 ± 1.1 Ma (Early Permian – Sakmarian to Artinskian). This age range is similar to the two high precision ^{40}Ar-^{39}Ar biotite ages determined from lamprophyric lavas at Killerton and Knowle Hill (290 ± 0.8 Ma and 281 ± 0.8 Ma, respectively; Edwards & Scrivener 1999) 100 km to the east, at the base of the post-Variscan Exeter Group succession in the Crediton Graben (Edwards *et al.* 1997).

Three dykes dated occur to the south and east of the Carnmenellis Granite (Fig. 2) close to, respectively, the E-W striking trace of the extensionally reactivated Carrick Thrust along the Helford Estuary (NED01/NED03) and its ~N-S striking reactivated lateral ramp along the Fal Estuary (NED07/NED12; Alexander & Shail 1996). The oldest lamprophyre dyke, NED07 (Pendennis Point; 292.10 ± 1.5 Ma), overlaps in age with the oldest part of the Carnmenellis Granite (U-Pb monazite 293.1 ± 1.3 Ma, Chen *et al*. 1993). This relationship confirms that mantle and crustal-derived magmas were contemporaneous from the earliest stage of magmatism to at least 281.8 Ma (Knowle Hill lava; Edwards & Scrivener 1999). Interactions between mantle and crustal melts are supported by the mafic enclave compositions (Stimac *et al.* 1995) and whole rock geochemical and isotopic signatures (Darbyshire & Shepherd 1994) of the Cornubian Batholith and the He isotope systematics of associated magmatic-hydrothermal mineralisation (Shail *et al.* 2003).

Although published maps suggest samples NED01 and NED03 are from the same intrusion, based on their relative proximity and orientations, there is a > 3 Ma difference in the phlogopite ages of these two samples that cannot be fully explained by analytical error (2σ). This difference suggests that NED01 and NED03 may in fact be separate intrusions and that magma injection into the extensionally reactivated Carrick Thrust fault system occurred in multiple stages, separated by up to a few million years. Alternatively, the two samples may be from the same composite intrusion, emplaced during multiple phases of magma injection. The latter is supported by the presence of small (2-10 cm) xenoliths of lamprophyric material, observed in some dykes (e.g. Smith 1929), including NED01. A two-stage emplacement history has also been suggested for the Fremington lamprophyre dyke (Roberts 1997).

Post-Variscan fracture-controlled hydrothermal activity, associated with: (i) incremental emplacement of the Cornubian Batholith and concomitant release of magmatic-hydrothermal fluids *c.* 295-259 Ma (e.g. Halliday *et al.* 1980; Shepherd & Darbyshire 1986; Chesley *et al*. 1991; Chesley *et al.* 1993; Chen *et al.* 1993) and (ii) migration of 'cross-course' basinal brines *c.* 240-220 Ma (Scrivener *et al.* 1994; Jackson *et al.* 1982) occurs widely in SW England. NED04 crops out in Holywell Bay, approximately 1 km NE of Wheal Golden, which worked Pb-Ag mineralization (Dines 1956), associated with the latter event. The whole rock $^{40}Ar/Ar^{39}$ age of *c.* 262 Ma from this sample is significantly younger than the cooling age of phlogopites in other lamprophyres. We therefore interpret this younger age to reflect post-

emplacement hydrothermal activity that contributed to the formation of observed secondary sericite, calcite, dolomite and some iron carbonates.

Late Carboniferous-Early Permian lamprophyre-granite emplacement and mineralization is common to several regions of the European Variscides (Fig. 1) including the Rhenohercynian and Saxothuringian Zones of the Bohemian Massif (*c.* 334-323 Ma and *c.* 297-295 Ma; von Seckendorff *et al.* 2004; Hegner *et al.* 1998), the Central Iberian Zone of the Iberian Massif (*c.* 265 Ma; Scarrow *et al.* 2011; Orejana *et al.* 2008; Bea *et al.* 1999) and the Variscan basement of the Alps (*c.* 290 Ma; Bussien *et al.* 2008). Lamprophyres throughout the Variscides share several common features, including i) Late Carboniferous-Early Permian emplacement ages concurrent with extensional and/or transtensional tectonics (Vaughan & Scarrow 2003; Shail & Wilkinson 1994), (ii) geochemical and isotopic signatures characteristic of a previously metasomatized sub-continental lithospheric mantle source (Scarrow *et al.* 2011), and (iii) an association in space and time with voluminous intermediate-felsic batholiths (e.g. Bea *et al.* 1999; von Seckendorff *et al.* 2004). These similarities suggest that the processes responsible for post-collisional magma generation and emplacement in various parts of the orogen are genetically linked. Coeval lamprophyres, basalts and granites in SW England are therefore likely a local expression of a much larger tectonothermal event that affected several regions of the European Variscides at the end of the Variscan orogeny.

A transition from convergent to extensional/transtensional tectonics during the latest Carboniferous is recorded throughout most of NW Europe (e.g. Arthaud and Matte 1977; Henk 1999; Wilson *et al.* 2004; Ziegler and Dèzes 2006). More generally, the generation of mafic magmas in a post-collisional setting has been attributed to asthenospheric upwelling caused by: (i) extensional tectonics, that may, or may not, be associated with orogenic collapse (e.g. Seyitoğlu & Scott 1996), (ii) lithospheric delamination (Gutierrez-Alonso et al. 2011), or (iii) slab breakoff (e.g. Dilek & Altunkaynak 2009).

Extension in SW England is unlikely to be driven by orogenic collapse as there is little evidence for substantial crustal thickening and subsequent exhumation of high-grade metamorphic rocks. Extension of previously-thickened lithosphere due to latest Carboniferous changes in plate boundary stresses is a viable alternative (Henk, 1997; 1999) that is broadly synchronous with intraplate extensional and transtensional rift processes operating across the post-Variscan foreland (Wilson *et* al. 2004; Timmermann *et* al. 2009). The distinction between changing plate boundary stresses, lithospheric delamination and slab detachment is problematical as all can result in lithospheric thinning, asthenosphere upwelling, partial melting, bimodal magmatism, uplift and extension centered on the suture zone. However, approximately 60 Ma separates the earliest Carboniferous closure of the Rhenohercynian Ocean (e.g. Holder & Leveridge 1986a) and the onset of Early Permian post-Variscan magmatism in SW England and this is longer than would be normally expected for slab break-off (e.g. Pe-Piper et al. 2009). Post-convergence

delamination in the suture zone remains a possibility but, if so, its timing may be more appropriately explained by delamination following the late development of the Cantabrian Orocline (Gutierrez Alonso et al., 2011; Fernandez Suarez et al., 2014), although SW England is somewhat distant. In addition, there is the possibility that the formation of Pangea resulted in the widespread occurrence of anomalous asthenospheric temperatures (e.g. Doblas *et al.* 1998). It is beyond the geochronological focus of this study to further distinguish between the above mechanisms.

Conclusions

1. Four lamprophyre dykes to the south and east of the Carnmenellis granite, south Cornwall, yielded Ar-Ar phlogopite cooling ages between 292.10 ± 1.5 Ma and 284 ± 1.1 Ma (Early Permian – Sakmarian to Artinskian).
2. These cooling ages are interpreted to reflect post-collisional lamprophyre emplacement ages and, combined with geochronological data from the nearby Carnmenellis pluton (293.1 ± 1.3 Ma; Chen *et al.* 1993), indicates that mantle- and more voluminous crustal-derived magmatism was contemporaneous from at least *c.* 292 Ma to *c.* 281 Ma.
3. The lamprophyres and granites of SW England may be a local expression of a regional, *c.* 300-280 Ma tectonothermal event(s) that resulted in similar and coeval magmatism in several locations the European Variscides. The processes responsible for this extensive magmatism require further investigation.

References

Alexander, A.C., Shail R.K. 1996. Late- to post-Variscan structures on the coast between Penzance and Pentewan, south Cornwall. *Proceedings of the Ussher Society*, **9**, 72-78.

Arenas, R., Díez Fernández, R., Sánchez Martínez, S., Gerdes, A., Fernández-Suárez, J. & Albert, R. 2014. Two-stage collision: Exploring the birth of Pangea in the Variscan terranes. *Gondwana Research*, **25,** 756-763.

Arthaud, F. & Matte, P. 1977. Late Palaeozoic strike-slip faulting in southern Europe and northern Africa: Result of a right-lateral shear zone between the Appalachians and the Urals. *Bulletin of the Geological Society of America,* **88,** 1305-1320.

Atherton, M.P. & Ghani, A.A. 2002. Slab breakoff: A model for Caledonian, Late Granite syn-collisional magmatism in the orthotectonic (metamorphic) zone of Scotland and Donegal, Ireland. *Lithos*, **62**, 65–85.

Bea, F., Montero, P. & Molina, J.F. 1999. Mafic precursors, peraluminous granitoids, and late lamprophyres in the Avila Batholith: A model for the generation of Variscan batholiths in Iberia. *Journal of Geology,* **107**(4), 399-419.

Bussien, D., Bussy, F., Masson, H., Magna, T. & Rodionov, N. 2008. Variscan lamprophyres in the Penninic domain (Central Alps): age and tectonic significance. *Bulletin de la Société Géologique de France,* **179**(4), 369-381.

Chen, Y., Clark, A., Farrar, E., Wasteneys, H., Hodgson, M. & Bromley, A., 1993. Diachronous and independent histories of plutonism and mineralization in the

Cornubian Batholith, southwest England. *Journal of the Geological Society of London,* **150**, 1183-1191.

Chesley, J.T., Halliday, A.N., Snee, L.W., Mezger, K., Shepherd, T.J. & Scrivener, R.C., 1993. Thermochronology of the Cornubian batholith in southwest England: Implications for pluton emplacement and protracted hydrothermal mineralization. *Geochimica et Cosmochimica Acta,* **57**, 1817-1837.

Chesley, J.T., Halliday, A.N. & Scrivener, R.C. 1991. Sm-Nd direct dating of fluorite mineralization. *Science,* **252**, 949-951.

Clark, A.H., Chen, Y., Farrar, E., Northcote, B., Wastenays, H.A.H.P, Hodgson, M.J. & Bromley, A. 1994. Refinement of the time/space relationships of intrusion and hydrothermal activity in the Cornubian Batholith (abstract). *Proceeedings of the Ussher Society*, **8**, 345.

Clark, A.H., Sandeman, H.A., Liu, C., Scott, D.J., Farrar, E., Archibald, D.A., Bromley, A.V., Jones, K.A. & Warr, L.N. 1998. An emerging geochronological record of the construction and emplacement of the Lizard ophiolite, SW Cornwall. *Geoscience of South-West England*, **9**, 276–277.

Dalrymple, G.B., Alexander, Jr., E.C., Lanphere, M.A. & Kraker, G.P. 1981. Irradiation of samples for $^{40}Ar/^{39}Ar$ dating using the Geological Survey TRIGA Reactor. U.S. Geological Survey, Professional Paper, **1176**.

Darbyshire, D.P.F. & Shepherd, T.J. 1994. Nd and Sr isotope constraints on the origin of the Cornubian batholith, SW England. *Journal of the Geological Society of London*, **151**, 795-802.

Deer, W. A., Howie, R. A., & Zussman, J. 1992. *An introduction to the rock-forming minerals* (Vol. 2). Longman Scientific & Technical, Hong Kong.

Dines, H.G. 1956. *The metalliferous mining region of south-west England.* Economic Memoir of the Geological Survey of Great Britain.

Di Vincenzo, G., Viti, C. & Rocchi, S. 2003. The effect of chlorite interlayering on ^{40}Ar-^{39}Ar biotite dating: an ^{40}Ar-^{39}Ar laser probe and TEM investigation of variably chloritised biotites. *Contributions to Mineralogy and Petrology*, **145**, 643-658.

Doblas, M., Oyarzun, R., Lopez-Ruiz, J., Cebria, J.M., Youbi, N., Mahecha, V., Lago, M., Pocovi, A. & Cabanis, B. 1998. *Journal of African Earth Sciences,* **26,** 88-99.

Dodson, H.R. & Rex, D.C. 1971. Potassium–argon ages of slates and phyllites from south-west England. *Journal of the Geological Society of London*, **126**, 464–499.

Edwards, R.A. & Scrivener, R.C. 1999. Geology of the country around Exeter: Memoir for 1:50 000 Geological Sheet 325 (England and Wales).

Edwards, R.A., Warrington, G., Scrivener, R.C., Jones, N.S., Haslam, H.W. & Ault, L. 1997. The Exeter Group, south Devon, England: a contribution to the early post-Variscan stratigraphy of NW Europe. *Geological Magazine,* **134**, 177-197.

Floyd, P.A., Exley, C.S. & Styles, M.T. 1993. *Igneous Rocks of SW England.* Chapman & Hall, London.

Fortey, N.J. 1991. The Exeter Volcanic Rocks: petrology and mineralogy. British Geological Survey Technical Report, WG/91/35.

Fowler, M.B. & Henney, P.J. 1996. Mixed Caledonian appinite magmas: implications for lamprophyre fractionation and high Ba–Sr granite genesis. *Contributions to Mineralogy and Petrology,* **126**, 199–215.

Franke, W. 1989. Tectonostratigraphic units in the Variscan belt of central Europe. *Geological Society of America,* Special Paper, **230**, 67-90.

Franke, W. 2000. The mid-European segment of the Variscides: tectonostratigraphic units, terrane boundaries and plate tectonic evolution, in: W. Franke, V. Haak, O. Oncken, D. Tanner (Eds.), Orogenic processes: Quantification and modelling in the Variscan Belt, Geol. Soc. Lond. Spec. Publ. 179, 35-61.

Fernandez-Suarez, J., Gutiérrez-Alonso, G., Johnston, S.T., Jeffries, T.E., Pastor-Galan, D., Jenner, G.A., & Murphy, J.B., 2011. Iberian late Variscan granitoids: some consideration on crustal sources and "mantle extraction ages". *Lithos*, **123**, 121-132.

Grimmer, S.C. and Floyd, P.A. 1986. Geochemical features of Permian rift volcanism – a comparison of Cornubian and Oslo basic volcanics. *Proceedings of the Ussher Society*, **6**, 352-359.

Gutiérrez-Alonso, G., Murphy, J.B., Fernández-Suárez, J., Piedad Franco, M., Carlos Gonzalo, J, & Weil, A.B., 2011a. Lithospheric mantle replacement in the core of Pangea: Sm-Nd insights from Iberia. *Geology*, **39**, 155-158.

Gutiérrez-Alonso, G., Fernández-Suárez, J., Jeffries, T.E., Johnston, S.T., Pastor-Galán, D., & Murphy, J.B., 2011b. Piedad Franco, M., Carlos Gonzalo, J., Post-tectonic granitoids of Iberia in time and space. *Tectonics*, **30**, TC5008, DOI: 10.1029/2010TC002845.

Hall, A. 1982. The Pendennis peralkaline minette. *Mineralogical Magazine,* **45**, 257-266.

Halliday, A.N. 1980. The timing of early and main stage ore mineralization in southwest Cornwall. *Economic Geology*, **75,** 752-759.

Hawkes, J.R. 1981. A tectonic 'watershed' of fundamental consequence in the post-Westphalian evolution of Cornubia. *Proceedings of the Ussher Society,* **5**, 128-131.

Hegner, E., Kölbl-Ebert, M. & Loeschke, J. 1998. Post-collisional lamprophyres (Black Forest, Germany): $^{40}Ar/^{39}Ar$ phlogopite dating, Nd, Pb, Sr isotope, and trace element characteristics. *Lithos,* **45**, 395-411.

Henk, A. 1997. Gravitational orogenic collapse vs plate-boundary stresses: a numerical modelling approach to the Permo-Carboniferous evolution of Central Europe. *Geologische Rundschau,* **86,** 39-55.

Henk, A. 1999. Did the Variscides collapse or were they torn apart?: A quantitative evaluation of the driving forces for postconvergent extension in central Europe. *Tectonics,* **18,** 774-792.

Holder, M.T. & Leveridge, B.E. 1986a. A model for the tectonic evolution of south Cornwall. *Journal of the Geological Society of London*, **143**, 125-134.

Holder, M.T. & Leveridge, B.E. 1986b. Correlation of the Rhenohercynian Variscides. *Journal of the Geological Society of London,* **143**, 141-147.

Hollick, L.M., Scrivener, R.C. and Burt, C.E. 2014. Geology of the Newquay district — a brief explanation of the geological map. *Sheet Explanation of the British Geological Survey.* 1:50 000 Sheet 346 Newquay (England and Wales).

Jackson, N.J., Halliday, A.N., Sheppard, S.M.F. & Mitchell, J.G. 1982. Hydrothermal activity in the St. Just mining district, Cornwall, England. In: *Metallization*

associated with acid magmatism (eds) Evans, A.M. John Wiley & Sons, London, 137-139.

Jourdan, F., Féraud, G., Bertrand, H., Watkeys, M.K., Renne, P.R. 2008. The $^{40}Ar/^{39}Ar$ ages of the sill complex of the Karoo large igneous province: Implications for the Pliensbachian-Toarcian climate change. *Geochemistry, Geophysics, Geosystems,* **9**(6), DOI: 10.1029/2008GC001994.

Kuiper, Y.D. 2003. The interpretation of inverse isochron diagrams in $^{40}Ar/39$ Ar geochronology. *Earth and Planetary Science Letters,* **203**(1), 499-506.

Leat, P.T., Thompson, R.N., Morrison, M.A., Hendry, G.L. & Trayhorn, S.C. 1987. Geodynamic significance of post-Variscan intrusive and extrusive potassic magmatism in SW England. *Transactions of the Royal Society of Edinburgh: Earth Sciences*, **77**, 349-360.

Leveridge, B.E. 2011. The Looe, South Devon and Tavy basins: the Devonian rifted passive margin successions. *Proceedings of the Geologists' Association,* **122**, 616-717.

Leveridge, B.E. & Hartley, A.J. 2006. The Variscan Orogeny: the development and deformation of Devonian/Carboniferous basins in SW England and South Wales. *In*: Brenchley, P.J. & Rawson, P.F. (eds) The Geology of England and Wales. *Geological Society of London*, Special Publication, 225-255.

Leveridge, B.E. & Shail, R.K. 2011. The Gramscatho Basin, south Cornwall, UK: Devonian active margin successions. *Proceedings of the Geologists' Association*, **122**(4), 568-615.

Ludwig, K.R. 2008. User's Manual for ISOPLOT 3.60 - A Geochronological Toolkit for Microsoft Excel. *Berkeley Geochronological Centre,* Special Publication, **4**, 54.

Matte, P. 2001. The Variscan collage and orogeny (480-290 Ma) and the tectonic definition of the Armorica microplate: a review. *Terra Nova,* **13**, 122-128.

McDougall, I. & Harrison, T.M. 1988. Geochronology and thermochronology by the $^{40}Ar/^{39}Ar$ Method. *Oxford University Press*, N.Y., 212.

Miller, J.A., Shibata, K. & Munro, M. 1962. The Potassium-Argon Age of the Lava of Killerton Park, Near Exeter. *Geophysical Journal*, **6**, 394-396.

Nance, R.D., Neace, E.R., Braid, J.A., Murphy, J.B., Dupuis, N. 2015. Does the Meguma Terrane extend into SW England? *Geoscience Canada,* **41**, http://www.dx.doi.org/10.12789/geocanj.2014.41.056.

Nance, R.D., Gutiérrez-Alonso, G., Keppie, J.D., Linnemann, U., Murphy, J.B., Quesada, C., Strachan, R.A., & Woodcock, N.H. 2010. Evolution of the Rheic Ocean. *Gondwana Research,* **17**, 194-222.

Onstott, T.C., Phillips, D. & Pringle-Goodell, L. 1991. Laser microprobe measurement of chlorine and argon zonation in biotite. *Chemical Geology,* **90**, 145-168.

Orejana, D., Villaseca, C., Billström, K. & Paterson, B.A. 2008. Petrogenesis of Permian alkaline lamprophyres and diabases from the Spanish Central System and their geodynamic context within western Europe. *Contributions to Mineralogy and Petrology,* **156**(4), 477-500.

Paine, J.H., Nomade, S. & Renne, P.R. 2006. Quantification of ^{39}Ar recoil ejection from GA1550 biotite during neutron irradiation as a function of grain dimensions. *Geochimica et Cosmochimica Acta,* **70**, 1507-1517.

Renne, P.R., Swisher, C.C., Deino, A.L., Karner, D.B., Owens, T.L., & DePaolo, D.J. 1998. Intercalibration of standards, absolute ages and uncertainties in ^{40}Ar-^{39}Ar dating. *Chemical Geology*, **145**, 117-152.

Roberts, C.L. 1997. The petrography of the Fremington dyke. *Proceedings of the Ussher Society*, **9**, 182-187.

Roddick, J.C. 1983. High precision intercalibration of $^{40}Ar/^{39}Ar$ standards. *Geochimica et Cosmochimica Acta*, **47**, 887-898.

Rundle, C C. 1980. K-Ar ages for lamprophyre dykes from SW England. Institute of Geological Sciences, Isotope Geology Unit Report, No. 80/9.

Rundle, C C. 1981. K-Ar ages for micas from SW England. Institute of Geological Sciences, Isotope Geology Unit Report, No. 81/10.

Scarrow, J.H., Molina, J.F., Bea, F., Montero, P. & Vaughan, A.P.M. 2011. Lamprophyre dykes as tectonic markers of late orogenic transtension timing and kinematics: A case study from the Central Iberian Zone. *Tectonics,* **30**, doi:10.1029/2010TC002755, 2011.

Scrivener, R.C., Darbyshire, D.P.F. & Shepherd, T.J. 1994. Timing of significance of cross-course mineralization in SW England. *Journal of the Geological Society of London,* **150**, 587-590.

Shail, R.K. & Leveridge, B.E. 2009. The Rhenohercnian passive margin of SW England: development, inversion and extensional reactivation. *Comptes Rendus Geoscience*, **341**, 140-155.

Shail, R.K., Stuart, F.M., Wilkinson, J.J. & Boyce, A.J. 2003. The role of post-Variscan extensional tectonics and mantle melting in the generation of the Lower

Permian granites and the giant W-As-Sn-Cu-Zn-Pb orefield of SW England (extended abstract). *Applied Earth Science (Transactions of the Institution of Mining and Metallurgy: Section B),* **112**, 127-129.

Shail, R.K. & Wilkinson, J.J. 1994. Late- to post-Variscan extensional tectonics in south Cornwall. *Proceedings of the Ussher Society*, **8**, 162-270.

Shepherd, T.J. & Darbyshire, D.P.F. 1986. Fluid inclusion and Rb-Sr geochronology of mineral deposits. In: Nesbitt, R.W. & Nichol I. (eds) *Geology in the Real World, Institution of Mining and Metallurgy*, Kingsley Dunham Volume, 403-412.

Smith, H.G. 1929. Some features of Cornish lamprophyres. *Proceedings of the Geologists' Association*, **40**, 260-268

Steiger, R.H. & Jäger, E. 1977. Subcommission on geochronology: Convention on the use of decay constants in geo- and cosmo-chronology. *Earth and Planetary Science Letters*, **36**, 359-362.

Stimac, J.A., Clark, A.H., Chen, Y., & Garcia, S. 1995. Enclaves and their bearing on the origin of the Cornubian batholith, southwest England. *Mineralogical Magazine*, **59**, 273-296.

Strachan, R.A., Linnemann, U., Jeffries, T., Drost, K., & Ulrich, J. 2013. Armorican provenance for the mélange deposits below the Lizard ophiolite (Cornwall, UK): evidence for Devonian obduction of Cadomian and Lower Palaeozoic crust onto the southern margin of Avalonia. *International Journal of Earth Sciences*, DOI 10.1007/s00531-013-0961-x.

Thorpe, R.S., Cosgrove, M.E. & Van Calsteren, P.W.C. 1986. Rare earth element, Sr- and Nd-isotope evidence for petrogenesis of Permian basaltic and K-rich

volcanic rocks from SW England. *Mineralogical Magazine*, **50**, 481-90

Tidmarsh, W.G. 1932. The Permian Lavas of Devon. *Quarterly Journal of the Geological Society*, **88,** 712-775.

Vaughan, A.P.M. & Scarrow, J.H. 2003. K-rich mantle metasomatism control of localization and initiation of lithospheric strike-slip faulting. *Terra Nova,* **15**, 163-169.

Von Seckendorff, V., Timmerman, M.J., Kramer, W. & Wobel, P. 2004. New $^{40}Ar/^{39}Ar$ ages and geochemistry of late Carboniferous-early Permian lamprophyres and related volcanic rocks in the Saxothuringian Zone of the Variscan Orogen (Germany). *Geological Society, London, Special Publications,* **223**, 335-359.

Warr, L.N., Primmer T.J. & Robinson D. 1991. Variscan very low-grade metamorphism in southwest England: a diathermal and thrust-related origin. *Journal of Metamorphic Geology*, **9**, 751-764.

Warrington, G. & Scrivener, R.C. 1990. The Permian of Devon, England. *Review of Palaeobotany and Palynology,* **66,** 263-272.

Waters, C.N., Somerville, I.D., Jones, N.S., Cleal, C.J., Collinson, J.D., Waters, R.A., Besly, B.M., Dean, M.T., Stephenson, M.H., Davies, J.R., Freshney, E.C., Jackson, D.I., Mitchell, W.I., Powell, J.H., Barclay, W.J., Browne, M.A.E., Leveridge, B.E., Long, S.L. & McLean, D. 2011. *A revised correlation of Carboniferous rocks in the British Isles.* Geological Society of London Special Report, 26.

Wilson, M., Neumann, E–R., Davies, G.R., Timmerman, M.J., Heeremans, M. & Larsen, B.T. (editors). 2004. *Permo-Carboniferous Magmatism and Rifting in Europe.* Geological Society of London, Special Publication, No. 223.

Ziegler, P.A. & Dèzes, P. 2006. Crustal evolution of Western and Central Europe. In Gee, D.G. & Stephenson, R.A. (eds.) *European Lithosphere Dynamics.* Geological Society of London Memoir, **32,** 43–56

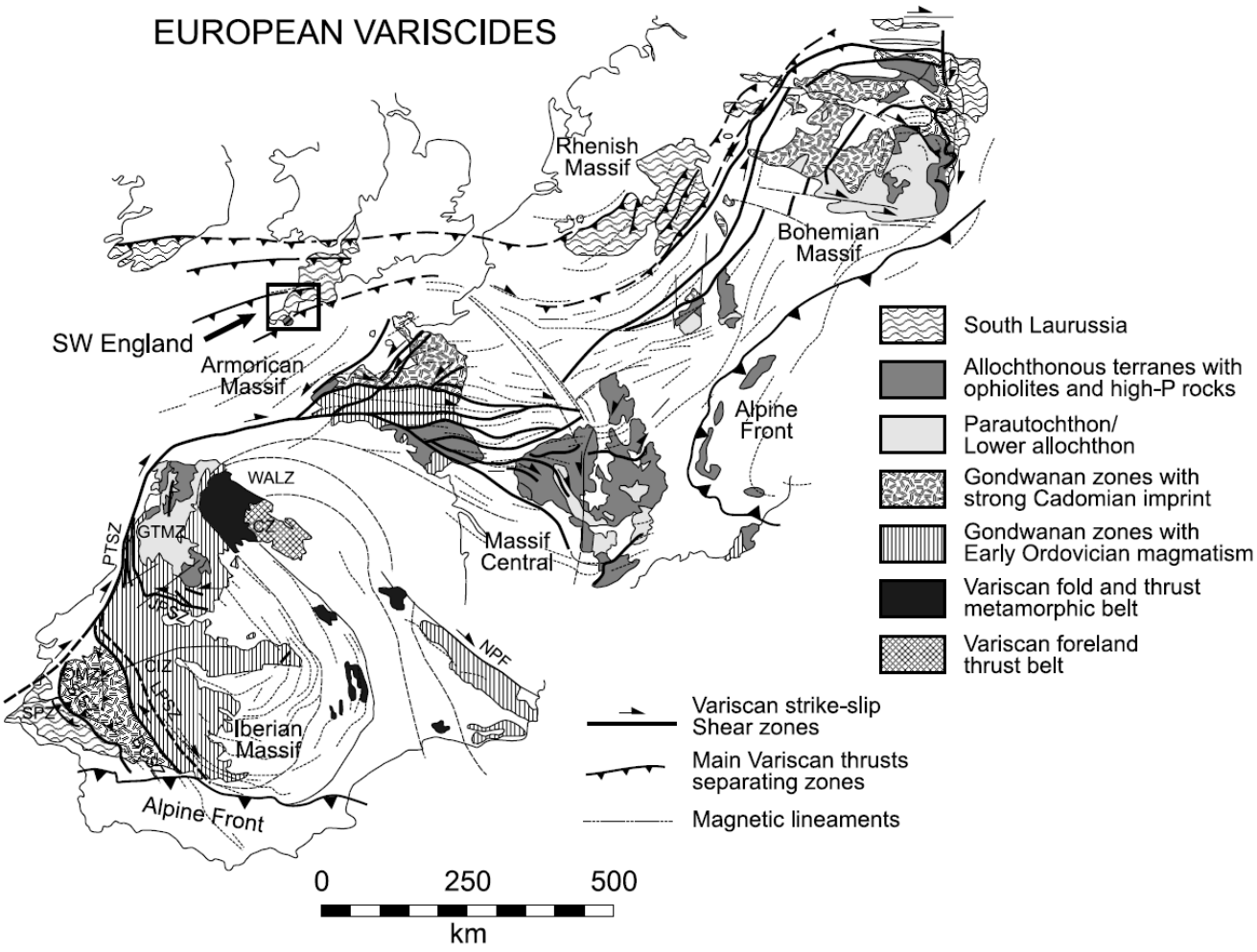

Fig. 1. Tectonostratigraphic zonation of the Variscan orogen of western Europe (modified from Martinez-Catalan et al. 2011). SPZ, South Portuguese Zone; OMZ, Ossa Morena Zone; CIZ, Central Iberian Zone; CZ, Cantabrian Zone; GTMZ, Galicia-Tras-os-Montes Zone; WALZ, West Asturian-Leonese Zone; NPF, North Pyrenean Fault; PTSZ, Porto-Tamar Shear Zone; LPSZ, Los Pedroches Shear Zone; JPSZ, Juxbado-Penalda Shear Zone; SISZ, Southern Iberian Shear Zone.

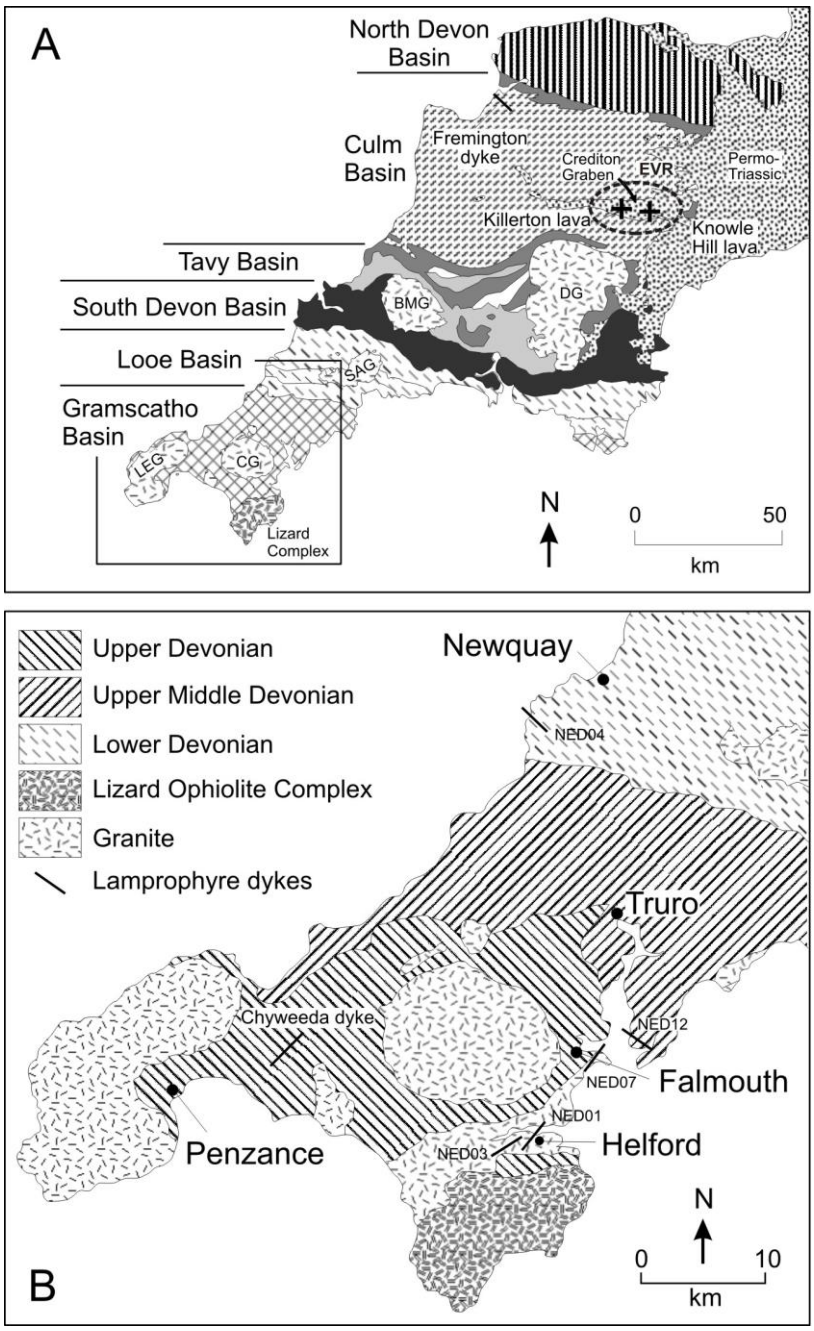

Fig. 2 (**a**) Simplified geological map of SW England (after Shail & Leveridge 2009). Previously dated lamprophyre occurrences are indicated by location names: Fremington (Roberts 1997), Killerton and Knowle Hill (Edwards & Scrivener 1999). General location of Exeter Volcanic Rocks (EVR) is indicated by dashed circle. (**b**) Simplified geological map of study area indicated by box in (a) showing sample locations (this study) indicated by sample names. Previously dated lamprophyre occurrence is indicated by location name: Chyweeda (Hawkes 1980). Corresponding ages for all lamprophyres are provided in Table 1. Note lamprophyre dykes on map are not to scale.

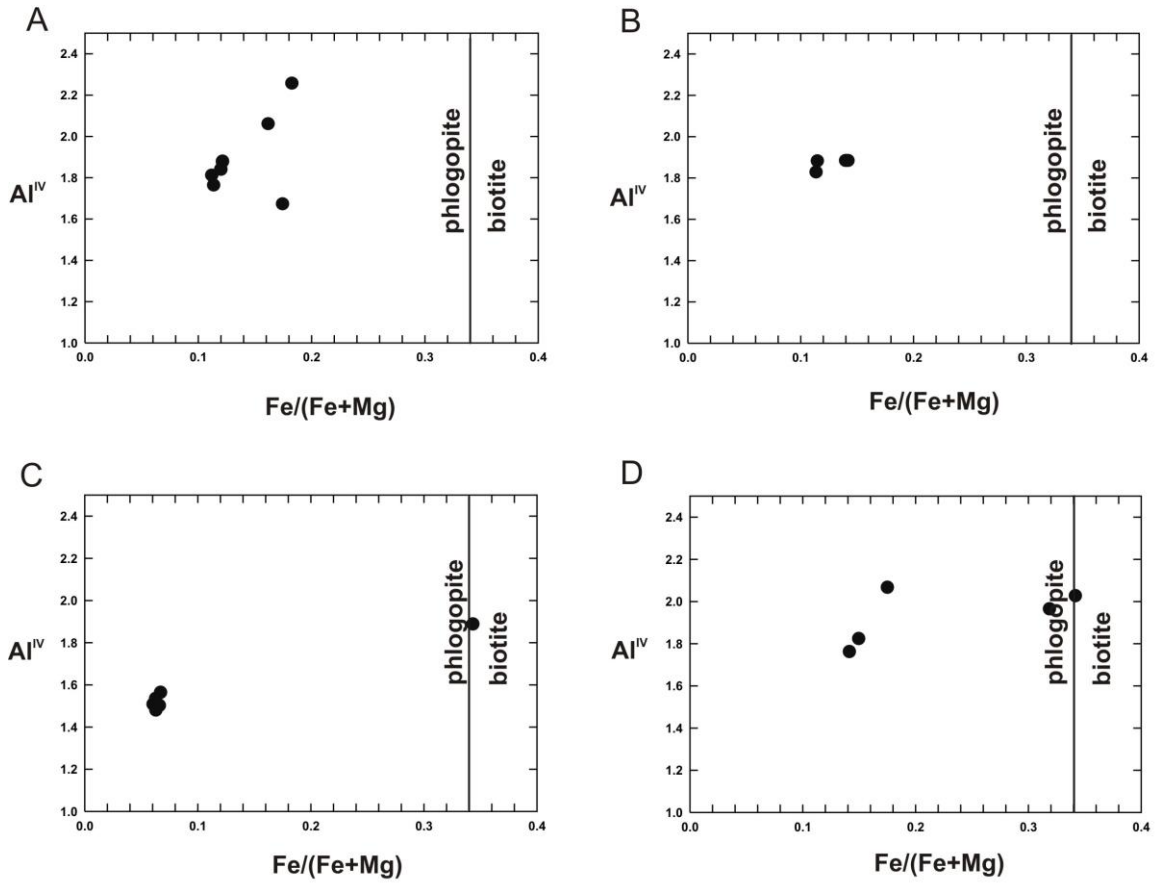

Fig. 3 Mica classification on the basis of Mg# and Al^{IV}, after Deer *et al.* 1992. (**a**) NED01. (**b**) NED03. (**c**) NED07. (**d**) NED12.

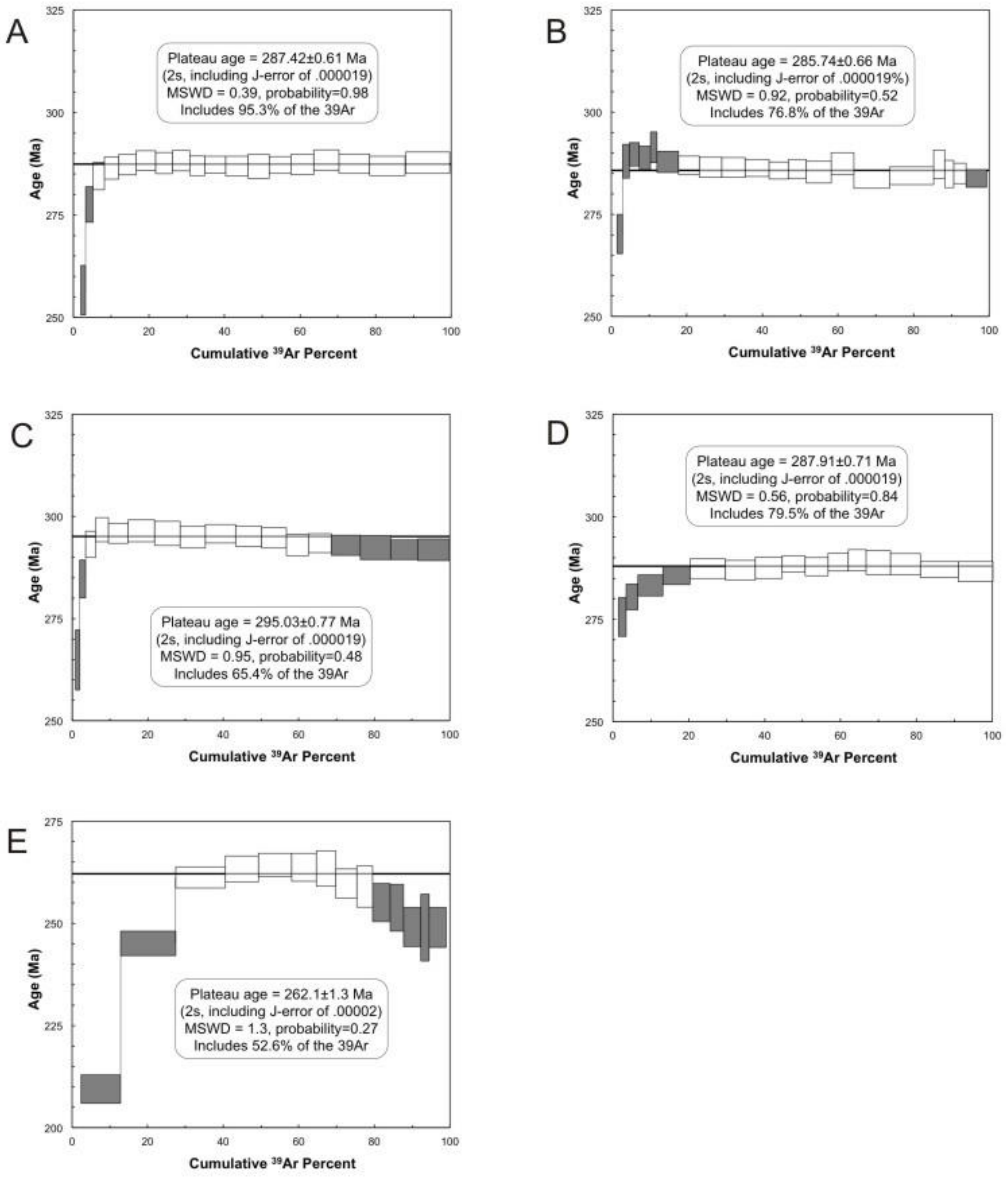

Fig. 4 $^{40}Ar/^{39}Ar$ plateau diagrams. Plateau segments are white; rejected steps are grey. (**a**) NED01 (phlogopite). B) NED03 (phlogopite). C) NED07 (phlogopite). D) NED12 (phlogopite). E) NED04 (whole rock).

Table 1 Geochronological summary of post-collisional magmatism in SW England

Rock type	Location	Method	Age ± 2σ (Ma)	Authors
Lamprophyres				
Lamprophyre lava	Killerton	Ar-Ar biotite	290.8 ± 0.8	Chesley (1992)
Lamprophyre lava	Knowle Hill	Ar-Ar biotite	**281.8 ± 0.8**	Chesley (1992)
Lamprophyre dyke	Fremington	Ar-Ar plagioclase	**292.4 ± 7.1**	Roberts (1997)
Lamprophyre dyke	Helford	Ar-Ar phlogopite		this study
Lamprophyre dyke	Fisherman's Creek.	Ar-Ar phlogopite		this study
Lamprophyre dyke	Pendennis Point	Ar-Ar phlogopite		this study
Lamprophyre dyke	Trelissick	Ar-Ar phlogopite		this study
Cornubian Batholith				
Land's End Granite	Lamorna Cove Quarry	U-Pb monazite	274.7 ± 0.4	Clark et al. (1994)
Land's End Granite	Newmill Quarry	U-Pb monazite	274.8 ± 0.5	Chesley et al. (1993)
Land's End Granite	Castle-an-Dinas Quarry	U-Pb monazite	276.7 ± 0.4	Clark et al. (1994)
Land's End Granite	Castle-an-Dinas Quarry	U-Pb xenotime	279.3 ± 0.4	Chesley et al. (1993)
Land's End Granite	Cripplesease	U-Pb monazite	277.1 ± 0.4	Clark et al. (1994)
Land's End Granite	Polgigga	U-Pb monazite	**274.4 ± 0.4**	Clark et al. (1994)
Carnmenellis/Carn Brea Granite	Carnsew Quarry	U-Pb monazite	293.1 ± 1.3	Clark et al. (1993)
Carnmenellis/Carn Brea Granite	Carnsew Quarry	U-Pb monazite	**293.7 ± 0.6**	Chesley et al. (1993)
Carnmenellis/Carn Brea Granite	Carn Brea	U-Pb monazite	292.0 ± 1.0	Clark et al. (1994)
Carnmenellis/Carn Brea Granite	Boswyn	U-Pb monazite	281.7 ± 0.8	Clark et al. (1994)
St. Austell Granite	Luxulyan Quarry	U-Pb monazite	280.6 ± 0.7	Clark et al. (1993)
St. Austell Granite	Luxulyan Quarry	U-Pb monazite	281.8 ± 0.4	Chesley et al. (1993)
Bodmin Moor Granite	Brockabarrow Common	U-Pb monazite	291.4 ± 0.8	Chesley et al. (1993)
Dartmoor Granite	Pewtor Quarry	U-Pb monazite	281.0 ± 0.6	Clark et al. (1994)
Dartmoor Granite	Haytor Quarry	U-Pb monazite	285.3 ± 0.6	Clark et al. (1994)
Dartmoor Granite	Yellowmeade Farm	U-Pb monazite	278.2 ± 0.8	Chesley et al. (1993)
Dartmoor Granite	Throwleigh Common	U-Pb monazite	286.2 ± 1.0	Clark et al. (1994)

Table 2. Summary of sample locations and structural information

Sample ID	OS Grid Ref.	BGS Map Sheet	Host Rock	Host Rock Age	Orientation	Ar-Ar Analysis
NED01	SW 753 265	359	Portscatho Fm.	Upper Devonian	040/30	Phl
NED03	SW 749 258	359	Portscatho Fm.	Upper Devonian	060/70	Phl
NED04	SW 766 601	346	Meadfoot Gr.	Lower Devonian	140/48	WR
NED07	SW 827 316	352	Portscatho Fm.	Upper Devonian	060/40	Phl
NED12	SW 834 387	352	Portscatho Fm.	Upper Devonian	318/20	Phl

Table 3. Summary of 40Ar–39Ar data

Sample	**NED01**	**NED03**	**NED04**	**NED07**	**NED12**
Mineral	Phl	Phl	WR	Phl	Phl
J	0.005608	0.005599	0.005625	0.005589	0.005617
± (1s)	0.000019	0.000019	0.000020	0.000019	0.000019
% error	0.34	0.34	0.36	0.34	0.34
high-T PSA*	287.59	284.38	248.90	292.10	286.90
± (2s)	0.68	1.07	3.20	1.50	1.54
with ± in J	1.93	2.08	3.60	2.40	2.36
MSWD	0.18	0.81	0.00	0.05	0.10
% 39Ar	88.43	35.38	11.33	23.79	19.04
PA**	287.42	285.74	262.10	295.00	287.91
± (2s)	0.61	0.66	1.30	0.80	0.71
with ± in J	n/a	n/a	n/a	n/a	n/a
MSWD	0.39	0.92	1.30	1.60	0.56
% 39Ar	95.30	76.80	52.60	65.40	79.50
CA***	288.00	284.90	n/a	292.40	289.30
± (2s)	2.10	2.00	n/a	3.20	0.71
with ± in J	n/a	n/a	n/a	n/a	n/a
MSWD	0.27	1.40	n/a	1.60	0.56
% 39Ar	95.30	97.30	n/a	94.30	100.00
Initial Ratio	248.00	445.00	n/a	477.00	232.00
Initial Ratio Err.	61.00	89.00	n/a	200.00	28.00